University of São Paulo
"Luiz de Queiroz" College of Agriculture

Mechanistic numerical modeling of solute uptake by plant roots

Andre Herman Freire Bezerra

Thesis presented to obtain the degree of Doctor of Science. Area: Agricultural Systems Engineering

Piracicaba
2014

Andre Herman Freire Bezerra
Bachelor in Agronomy

Mechanistic numerical modeling of solute uptake by plant roots

Supervisor:
Prof. Dr. **QUIRIJN DE JONG VAN LIER**

Thesis presented to obtain the degree of Doctor of Science. Area: Agricultural Systems Engineering

Piracicaba
2014

Ao passado,

ao presente e

ao futuro

Com amor, ***DEDICO***

ACKNOWLEDGEMENT

CONTENTS

ABSTRACT

Mechanistic numerical modeling of solute uptake by plant roots

Keywords:

RESUMO

Modelagem numérica de extração de solutos pelas raízes

Palavras-chave:

LIST OF FIGURES

LIST OF TABLES

1 INTRODUCTION

Analytical models of transport of nutrients in soil towards plant roots usually consider steady-state conditions with respect to flow of water due to the high nonlinearity of hydraulic functions. Several simplifications (assumptions) are made when solute uptake by the roots are taken into consideration, most of them also due to the nonlinearity of the influx rate function. Consequently, the analytical models, although describe the processes involved in the transport and uptake of solutes, are capable to simulate water and solute flow just for specific cases (simplified scenarios that most of the time are far from what happens in the field) and using them for situations that they were not designed for, is a rough approximation. Moreover, the analytical solutions have to use, at some point, numerical algorithms to compute results of some special functions (bessels, airys or infinite series, for example) that are part of the generated analytical expressions. Thus, for the case of convection-diffusion equation, even the fully analytical solutions are limited to some numerical estimation although they have yet fast and reliable results.

Numerical modeling, in turn, has more flexibility when dealing with nonlinear equations, being an alternative to surpass this problem. The functions can be solved considering transient conditions for water and solute flow but with some pull-backs like a greater concern about stability and higher time demanded to calculations. In general, the numerical models use empirical functions in the determination of osmotic stress, related to the electric conductivity in the soil solution. The parameters of these empirical models depend on soil, plant and atmospheric conditions in a range covered by the experiments that were made to generate data for the model calibration. One must be aware that using those models for different scenarios can result in errors not considered by the model itself and, most of the time, new calibration of the parameters needs to be done. A model that uses a mechanistic approach for the solute transport equations can describe the involved processes in a wider range of situations, since it is not dependent on experimental data, resulting in a more realistic solution.

In this work, a numerical mechanistic solution for the equation of convection–dispersion is proposed, assuming a soil concentration dependent solute uptake function as the boundary condition at root surface. The proposed model is compared with a no solute uptake and a constant solute uptake numerical models, and with an analytical model which uses steady-state condition for water content.

2 LITERATURE REVIEW

2.1 WATER FLOW

2.2 SOLUTE FLOW

2.2.1 MICHAELIS-MENTEN

2.3 NUMERICAL METHODS

3 METHODOLOGY

3.1 Michaelis-Menten equation

The solute flux density at root surface (q_{s0}) can be related to the Michaelis-Menten (MM) equation as the following:

$$q_{s0} = -D\frac{dC}{dr} + q_0 C \simeq \frac{I_m C_0}{K_m + C_0} + q_0 C_0 \tag{1}$$

where D ($m^2\ s^{-1}$) is the effective diffusion-dispersion coefficient; q_0 ($m^2\ s^{-1}$) is the water flux density at the root surface; I_m (mol $m^2\ s^{-1}$) and K_m (mol m^{-3}) are the MM parameters that represent the maximum solute uptake rate and the affinity of the plant to the solute type, respectively; and C_0 (mol m^{-3}) is the solute concentration in the soil solution at root surface.

We assume that the diffusive and convective parts of the original equation is similar to the active and passive uptakes of the MM equation, respectively, at root suurface. It is shown in Figure 0 XXX the two proposed partitioning of active and passive uptakes, for a constant water flux density. Figure 0a is linear, which is a simplification of MM equation to facilitate its use in the numerical solution. Figura 0a is the MM equation itself.

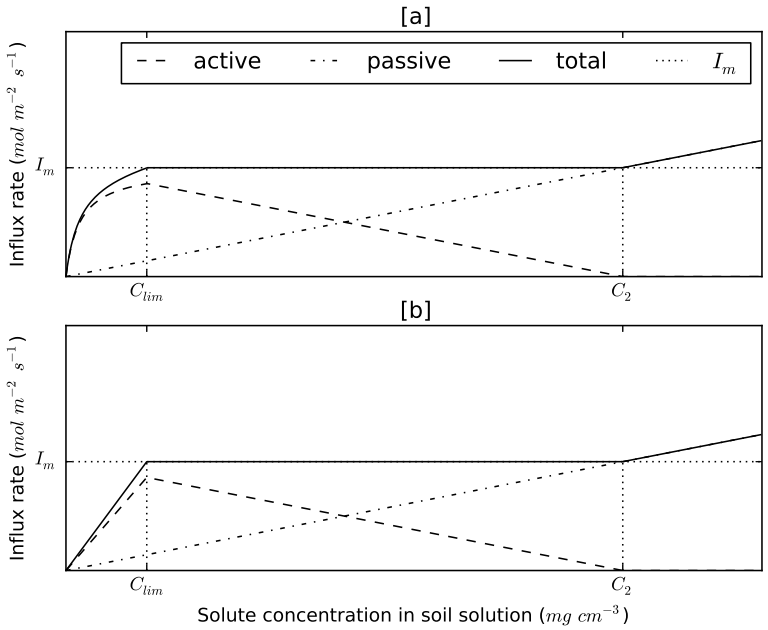

Figure 1 - Uptake (influx) rate as a function of concentration in soil water for [a] nonlinear case and [b] linear case

In the linearized equation (Figure 0b), the slope β of the total uptake line (continuous line), for concentration values smaller than C_{lim}, can be found by the relation $I_m/Clim$, since the line starts at the origin. According to the MM equation, for values

smaller than C_{lim}, the solute uptake is concentration dependent and the uptake is smaller than I_m. For values greater than C_2 the uptake is also concentration dependent but due to transport of mass by water flow only, i.e, active uptake is zero and the overall uptake is passive.

To find C_{lim}, we set the solute flux density to I_m:

$$I_m = \frac{I_m C_0}{K_m + C_0} + q_0 C_0 \ . \tag{2}$$

Solving for C, we find C_{lim}as the positive value of:

$$C_{lim} = -\frac{K_m \pm \left({K_m}^2 + 4 I_m K_m / q_0\right)^{1/2}}{2} \tag{3}$$

Finally, β can be defined as the positive value of:

$$\beta = -\frac{I_m}{C_{lim}} = -\frac{2 I_m}{K_m \pm \left({K_m}^2 + 4 I_m K_m / q_0\right)^{1/2}} \tag{4}$$

At concentration values greater than C_2, the solute uptake is driven only by mass flow of water and the active uptake is zero. Thus, C_2 can be found as:

$$C_2 = \frac{-I_m}{q_0} \tag{5}$$

The partitioning between active (α) and passive uptake (q_0) is done by difference, as the values of total uptake and passive uptake is always known:

$$\begin{aligned} &q_{s0} = (\text{active slope} + \text{passive slope})\, C_0 = \beta\, C_0 \\ &\text{passive slope} = q_0 \\ &\text{active slope} = \beta - q_0 = \alpha \\ &q_{s0} = (\alpha + q_0)\, C_0 \end{aligned} \tag{6}$$

The equation (6) is, therefore, the linearization of equation (1) for values of concentration smaller than C_{lim} and greater than C_2.

3.2 Water and solute transport equations

The water and solute differential equations for one-dimensional axisymetric flow were solved numerically and simulated iteratively as described in the following. The algorithm was based on the solution proposed by de Jong van Lier, Metselaar and van Dam (2006) and de Jong van Lier, van Dam and Metselaar (2009).

The Richards equation for one-dimensional axisymetric flow, assuming no sink or source and no gravitational component, can be written as:

$$\frac{\partial\theta}{\partial H}\frac{\partial H}{\partial t} = \frac{1}{r}\frac{\partial}{\partial r}\left(rK\frac{\partial H}{\partial r}\right) \tag{7}$$

where θ ($m^3\ m^{-3}$) is the water content, H (m) is the sum of pressure (h) and osmotic (h_π) heads, t (s) is the time, r (m) is the distance from the axial center and K ($m\ s^{-1}$) is the hydraulic conductivity.

Relations between K, θ and h are described by the van Genuchten equation system:

$$\Theta = [1 + |\alpha h|^n]^{(1/n)-1} = \frac{(\theta - \theta_r)}{(\theta_s - \theta_r)} \tag{8}$$

$$K = K_s\Theta^\lambda[1 - (1 - \Theta^{n/(n-1)})^{(1-(1/n))}]^2 \tag{9}$$

where θ_r and θ_s ($m^3\ m^{-3}$) are residual water content and saturated water content, respectively; α (m^{-1}), n and λ are empirical parameters.

The differential equation for convection-dispersion for transient one-dimensional axisymetric flow can be written as:

$$r\frac{\partial(\theta C)}{\partial t} = -\frac{\partial}{\partial r}\left(rqC\right) + \frac{\partial}{\partial r}\left(rD\frac{\partial C}{\partial r}\right) \tag{10}$$

where C ($mol\ m^{-3}$) is the solute concentration in the soil solution, q ($m\ s^{-1}$) is the water flux density and D ($m^2\ s^{-1}$) is the effective diffusion-dispersion coefficient.

The solute flux density at the outermost compartment (half distance between roots, i.e., $r = r_m$) is set to zero. The boundary conditions at innermost compartment (root surface, i.e, $r = r_0$) are set according to the model type, which are: no solute uptake model (de Jong van Lier, 2009), constant uptake model (de Willigen, 1994) and linear and nonlinear concentration–dependent model (proposed). For short, let us call them NU, CU, LU and NLU models, respectivelly.

For no solute uptake (NU) model type: the solute flux density is set to zero

$$q_{s0} = -D\frac{dC}{dr} + q_0C = 0 \tag{11}$$

For constant solute uptake (CU) model type: the solute flux density is set to the maximum and constant solute uptake rate I_m. For cylindrical coordinates, the solute flux density of each root is

$$q_{s0} = -D\frac{dC}{dr} + q_0 C = -\frac{I_m}{2\pi r_0 L} \tag{12}$$

where L (m) is the root length, r_0 (m) is the root radius and I_m has units of mol s^{-1}.

For linear concentration–dependent uptake (LU) model type: the solute flux density is set to the linearized piecewise MM equation

$$q_{s0} = -D\frac{dC}{dr} + q_0 C = -(\alpha + q_0)C_0 \tag{13}$$

For nonlinear concentration–dependent uptake (NLU) model type: the solute flux density is set to the MM equation

$$q_{s0} = -D\frac{dC}{dr} + q_0 C = -\left(\frac{I_m}{2\pi r_0 L(K_m + C_0)} + q_0\right) C_0 \tag{14}$$

3.3 Implicit numerical solution

The combined water and salt movement is simulated iteratively. In a first step, the water movement toward the root is simulated, assuming salt concentrations from the previous time step. In a second step, the salt contents per segment are updated and new values for the osmotic head in all segments are calculated. The first step is then repeated with updated values for the osmotic heads. This process is repeated until the pressure head values and osmotic head values between iterations converge. Two flowcharts with the algorithm procedures to solve water and solute iterative equations can be found in the Appendix.

3.3.1 Water

The implicit numerical discretization and the solution for the Eq. (7) was made according to de Jong van Lier et al. (2006), which has the following criteria:

(i) there is no sink (the only water exit is the root surface located at the inner side of the first compartment)

(ii) water flux density at the outermost compartment is set to zero

(iii) water flux density at the innermost compartment (at root surface) is set equal to water flux density entering the root, which is determined by transpiration rate and total root area

3.3.2 Solute

Fully implicit numerical discretization of Eq. (10) gives:

$$\theta_i^{j+1}C_i^{j+1} - \theta_i^j C_i^j = \frac{\Delta t}{2r_i\Delta r_i}\times \left\{ \frac{r_{i-1/2}}{r_i - r_{i-1}}\left[q_{i-1/2}(C_{i-1}^{j+1}\Delta r_i + C_i^{j+1}\Delta r_{i-1}) - 2D_{i-1/2}^{j+1}(C_i^{j+1} - C_{i-1}^{j+1})\right] - \frac{r_{i+1/2}}{r_{i+1} - r_i}\left[q_{i+1/2}(C_i^{j+1}\Delta r_{i+1} + C_{i+1}^{j+1}\Delta r_i) - 2D_{i+1/2}^{j+1}(C_{i+1}^{j+1} - C_i^{j+1})\right]\right\} \quad (15)$$

where $i\,(1 \le i \le n)$ is the segment number and j is the time step.

The boundary conditions at the root surface, for solutes, (inner boundary, $i = 1$) will be of zero, constant and concentration dependent solute flux, according to the models of de Jong van Lier (2009), de Willigen (1984) and proposed model, respectively.

The algorithm used in numerical simulations to solve Eq. (15) consist in finding C_i^{j+1} for each segment, which can be done by solving the tridiagonal matrix as follows

$$\begin{bmatrix} b_1 & c_1 & & & & \\ a_2 & b_2 & c_2 & & & \\ & a_3 & b_3 & c_3 & & \\ & & \ddots & \ddots & \ddots & \\ & & & a_{n-1} & b_{n-1} & c_{n-1} \\ & & & & a_n & b_n \end{bmatrix} \begin{bmatrix} C_1^{j+1} \\ C_2^{j+1} \\ C_3^{j+1} \\ \vdots \\ C_{n-1}^{j+1} \\ C_n^{j+1} \end{bmatrix} = \begin{bmatrix} f_1 \\ f_2 \\ f_3 \\ \vdots \\ f_{n-1} \\ f_n \end{bmatrix} \quad (16)$$

with $f_i(\mathrm{mol\ m^{-2}})$ defined, unless specified otherwise, as

$$f_i = r_i\theta_i^j C_i^j \quad (17)$$

and $a_i\,(\mathrm{m})$, $b_i\,(\mathrm{m})$ and $c_i\,(\mathrm{m})$ are defined according to the respective segments and model type as described in the following.

1. The intermediate nodes ($i = 2$ to $i = n - 1$) are the same for all models

   Rearrangement of Eq. (15) to eq. (16) results in the coefficients:

$$a_i = -\frac{r_{i-1/2}(2D_{i-1/2}^{j+1} + q_{i-1/2}\Delta r_i)\Delta t}{2(r_i - r_{i-1})\Delta r_i} \quad (18)$$

$$b_i = r_i\theta_i^{j+1} + \frac{\Delta t}{2\Delta r_i}\left[\frac{r_{i-1/2}}{(r_i - r_{i-1})}(2D_{i-1/2}^{j+1} - q_{i-1/2}\Delta r_{i-1}) + \frac{r_{i+1/2}}{(r_{i+1} - r_i)}(2D_{i+1/2}^{j+1} + q_{i+1/2}\Delta r_{i+1})\right] \quad (19)$$

$$c_i = -\frac{r_{i+1/2}\Delta t}{2\Delta r_i(r_{i+1} - r_i)}(2D_{i+1/2}^{j+1} - q_{i+1/2}\Delta r_i) \quad (20)$$

2. The outer boundary ($i = n$) is also the same for all models, which is of zero solute flux

Applying boundary condition of zero solute flux, the third and forth term from the right hand side of Eq. (15) are equal to zero. Thus, the solute balance for this segment is written as:

$$\theta_n^{j+1}C_n^{j+1} - \theta_n^j C_n^j = \frac{\Delta t}{2r_n \Delta r_n} \times \left\{ \frac{r_{n-1/2}}{r_n - r_{n-1}} \left[q_{n-1/2}(C_{n-1}^{j+1}\Delta r_n + C_n^{j+1}\Delta r_{n-1}) - 2D_{n-1/2}^{j+1}(C_n^{j+1} - C_{n-1}^{j+1}) \right] \right\} \quad (21)$$

Rearrangement of Eq. (21) to Eq. (16) results in the coefficients:

$$a_n = -\frac{r_{n-1/2}(2D_{n-1/2}^{j+1} + q_{n-1/2}\Delta r_n)\Delta t}{2(r_n - r_{n-1})\Delta r_n} \quad (22)$$

$$b_n = r_n\theta_n^{j+1} + \frac{\Delta t}{2\Delta r_n}\left[\frac{r_{n-1/2}}{(r_n - r_{n-1})}(2D_{n-1/2}^{j+1} + q_{n-1/2}\Delta r_{n-1}) \right] \quad (23)$$

3. The inner boundary ($i = 1$)

a) **Zero (no) uptake model (NU)**

Applying boundary condition of zero solute flux, the first and second term of the right-hand side of Eq. (15) are equal to zero:

$$\theta_1^{j+1}C_1^{j+1} - \theta_1^j C_1^j = \frac{\Delta t}{2r_1 \Delta r_1} \times \left\{ \frac{r_{1+1/2}}{r_2 - r_1} \left[-q_{1+1/2}(C_1^{j+1}\Delta r_2 + C_2^{j+1}\Delta r_1) + 2D_{1+1/2}^{j+1}(C_2^{j+1} - C_1^{j+1}) \right] \right\} \quad (24)$$

Rearrangement of Eq. (24) to Eq. (16) results in the following coefficients:

$$b_1 = r_1\theta_1^{j+1} + \frac{\Delta t}{2\Delta r_1}\left[\frac{r_{1+1/2}}{(r_2 - r_1)}(2D_{1+1/2}^{j+1} + q_{1+1/2}\Delta r_2) \right] \quad (25)$$

$$c_1 = -\frac{r_{1+1/2}\Delta t}{2\Delta r_1(r_2 - r_1)}(2D_{1+1/2}^{j+1} - q_{1+1/2}\Delta r_1) \quad (26)$$

b) **Constant uptake model (CU)**

Applying boundary conditions of constant solute flux, the first and second term of the right-hand side of Eq. (15) are equal to $-\frac{I_m}{2\pi r_0 L}\Delta r_1$ while $C > 0$:

$$\theta_1^{j+1}C_1^{j+1} - \theta_1^j C_1^j = \frac{\Delta t}{2r_1 \Delta r_1} \times \left\{ \frac{r_{1-1/2}}{r_1 - r_0} \left(-\frac{I_m}{2\pi r_0 L} \right) \Delta r_1 - \frac{r_{1+1/2}}{r_2 - r_1} \left[q_{1+1/2}(C_1^{j+1}\Delta r_2 + C_2^{j+1}\Delta r_1) - 2D_{1+1/2}^{j+1}(C_2^{j+1} - C_1^{j+1}) \right] \right\} \quad (27)$$

When $C = 0$ the maximum solute flux (I_m) is set to zero and the equation becomes equal to Eq. (24). Rearrangement of Eq. (27) to Eq. (16) results in the following coefficients:

$$b_1 = r_1\theta_1^{j+1} + \frac{\Delta t}{2\Delta r_1}\left[\frac{r_{1+1/2}}{(r_2 - r_1)}(2D_{1+1/2}^{j+1} + q_{1+1/2}\Delta r_2)\right] \tag{28}$$

$$c_1 = -\frac{r_{1+1/2}\Delta t}{2\Delta r_1(r_2 - r_1)}(2D_{1+1/2}^{j+1} - q_{1+1/2}\Delta r_1) \tag{29}$$

$$f_1 = r_1\theta_1^j C_1^j - \frac{r_{1-1/2}}{r_1 - r_0}I_m\frac{\Delta t}{4\pi r_0 L} \tag{30}$$

c) **Linear concentration dependent model (LU)**

Applying boundary conditions of linear concentration dependent solute flux, the first and second term of the right-hand side of Eq. (15) are equal to $-(\alpha + q_0)C_1^{j+1}\Delta r_1$ while $C < C_{lim}$ and $C > C_2$:

$$\theta_1^{j+1}C_1^{j+1} - \theta_1^j C_1^j = \frac{\Delta t}{2r_1\Delta r_1}\times$$
$$\left\{\frac{r_{1-1/2}}{r_1 - r_0}\left[-(\alpha + q_0)\right]C_1^{j+1}\Delta r_1 - \right. \tag{31}$$
$$\left.\frac{r_{1+1/2}}{r_2 - r_1}\left[q_{1+1/2}(C_1^{j+1}\Delta r_2 + C_2^{j+1}\Delta r_1) - 2D_{1+1/2}^{j+1}(C_2^{j+1} - C_1^{j+1})\right]\right\}$$

When $C = 0$ the solute flux is set to zero and the equation is equal to Eq. (24). While $C_{lim} \leq C \leq C_2$, the solute flux density is constant and the equation is equal to Eq. (27). Rearrangement of Eq. (31) to Eq. (16) results in the following coefficients:

$$b_1 = r_1\theta_1^{j+1} + \frac{\Delta t}{2\Delta r_1}\left[\frac{r_{1+1/2}}{(r_2 - r_1)}(2D_{1+1/2}^{j+1} + q_{i+1/2}\Delta r_2) - \frac{r_{1-1/2}}{r_1 - r_0}(\alpha + q_0)\Delta r_1\right] \tag{32}$$

$$c_1 = -\frac{r_{1+1/2}\Delta t}{2\Delta r_1(r_2 - r_1)}(2D_{1+1/2}^{j+1} - q_{1+1/2}\Delta r_1) \tag{33}$$

d) **Nonlinear concentration dependent model (NLU)**

Applying boundary conditions of nonlinear concentration dependent solute flux, the first and second term of the right-hand side of Eq. (15) are equal to $-(\frac{I_m}{2\pi r_0 L(K_m + C_1^{j+1})} + q_0)C_1^{j+1}\Delta r_1$ while $C < C_{lim}$ and $C > C_2$:

$$\theta_1^{j+1}C_1^{j+1} - \theta_1^j C_1^j = \frac{\Delta t}{2r_1\Delta r_1}\times$$
$$\left\{\frac{r_{1-1/2}}{r_1 - r_0}\left[-(\alpha + q_0)\right]C_1^{j+1}\Delta r_1 - \right. \tag{34}$$
$$\left.\frac{r_{1+1/2}}{r_2 - r_1}\left[q_{1+1/2}(C_1^{j+1}\Delta r_2 + C_2^{j+1}\Delta r_1) - 2D_{1+1/2}^{j+1}(C_2^{j+1} - C_1^{j+1})\right]\right\}$$

Rearrangement of Eq. (34) to Eq. (16) results in the following coefficients:

$$b_1 = r_1\theta_1^{j+1} + \frac{\Delta t}{2\Delta r_1}\left[\frac{r_{1+1/2}}{(r_2 - r_1)}(2D_{1+1/2}^{j+1} + q_{i+1/2}\Delta r_2) - \frac{r_{1-1/2}}{r_1 - r_0}\left(\frac{I_m}{2\pi r_0 L(K_m + C_1^{j+1})} + q_0\right)\Delta r_1\right] \tag{35}$$

$$c_1 = -\frac{r_{1+1/2}\Delta t}{2\Delta r_1(r_2 - r_1)}(2D_{1+1/2}^{j+1} - q_{1+1/2}\Delta r_1) \tag{36}$$

The value of C_1^{j+1} in Equation (35) is found using the iterative Newton-Raphson method. Note that since this is a one-dimensional microscopic model, it is assumed that the root has the same characteristcs in all vertical soil profile (along its vertical axis), thus, water and solute transport from soil towards the roots and uptakes are occurring at the same rate in the vertical profile. It is possible to couple this model in another one that has discretized soil layers. For a 2D model (depth and radial distance), the solutions presented here are applied in each layer independently. For a 1D model (only depth), an average of water and solute content through the horizontal profile has to be computed.

3.4 Linear and Nonlinear differences and statistics

To analyze the differences between the two proposed models (linear and nonlinear), the absolute and relative differences were calculated as follows:

$$diff_{abs} = \sum_{t=1}^{t_{end}} |CL_t - CNL_t| \tag{37}$$

$$diff_{rel} = \frac{\sum_{t=1}^{t_{end}} |CL_t - CNL_t|}{\sum_{t=1}^{t_{end}} CL_t} \tag{38}$$

where CL_t and CNL_t are the solute concentration in soil water for LU and NLU, respectvely, at a given time t, and t_{end} is the end time of the simulation.

The equations are the same of absolute and relative errors but since we are analyzing differences instead of errors (there is not a right or standard model), we called it differences.

Also, the Mann–Whitney U test was made with two datasets (concentration and cumulative uptake) for the two models. The choice of this test is due to the fact that the distributions for both datasets are not normal, the pairs (concentration for LU and for NLU and cumulative uptake for LU and NLU) are distinct and do not affect each

other. This test can decide whether each pair is identical without assuming them to follow the normal distribution (nonparametric test). The null hypothesis (H_0) is that both populations (model output data) are the same and the alternate hypothesis (H_1) is that one particular model (LU or NLU) has greater values than the other.

4 RESULTS AND DISCUSSION

The simulations were performed using the hydraulic parameters from the Dutch Staring series (WÖSTEN et al., 2001) for three typical top soils, as listed in Table 1. The general system parameters for the different scenarios are listed in Table 2 and values for the Michaelis-Menten parameters in Table 3. Values of root length density, salt content and relative transpiration were chosen to change, reflecting different possible scenarios that would occur in a practical situation. The chosen MM parameters were for K^+ solute.

Table 1 - Soil hydraulical parameters used in simulations

Staring soil ID	**Textural class**	**Reference in this paper**	$\boldsymbol{\theta_r}$ $m^3\,m^{-3}$	$\boldsymbol{\theta_s}$ $m^3\,m^{-3}$	$\boldsymbol{\alpha}$ m^{-1}	**l** –	**n** –	$\boldsymbol{K_s}$ $m\,d^{-1}$
B3	Loamy sand	Sand	0.02	0.46	1.44	-0.215	1.534	0.1542
B11	Heavy clay	Clay	0.01	0.59	1.95	-5.901	1.109	0.0453
B13	Sandy loam	Loam	0.01	0.42	0.84	-1.497	1.441	0.1298

Table 2 - System parameters used in simulations scenarios

Description	**Symbol**	**Scenario description**	**Value**	**Unit**
Root radius	r_0		0.5	mm
Limiting root potential	h_{lim}		-150	m
Root density	L	Low root density	0.01	cm cm^{-3}
		Medium root density	0.1	
		High root densit	1	
Half distance between roots	r_m	Low root density	56.5	mm
		Medium root density	17.8	
		High root densit	5.65	
Potential transpiration rate	T_p	Low	6	mm d^{-1}
		High	3	
Initial salt content in soil water	C_{ini}	Low	14	mol cm^{-3}
		High	140	
Diffusoin coefficient in water	$D_{m,w}$		$1.98\ 10^{-9}$	$m^2\ s^{-1}$
Dispersivity	τ		0.0005	m
Soil type		Sand	Table 1	
		Clay		
		Loam		

Table 3 - Michaelis-Menten parameters after Roose and Kirk (2009)

Solute	$\boldsymbol{I_m}$ mol m^{-2} s^{-1}	$\boldsymbol{K_m}$ mol m^{-3}
NO_3^-	$1\ 10^{-5}$	0.05
K^+	$2\ 10^{-6}$	0.025
$H_2PO_4^-$	$1\ 10^{-6}$	0.005
Cd^{2+}	$1\ 10^{-6}$	1

4.1 Linear versus nonlinear comparison

This section describes how the linear (LU) and nonlinear (NLU) solutions simulate the transport of water and solutes in the soil, plant and atmosphere system. The analysis of the results was made in order to choose one out of the two models in further simulations. The nonlinear solution uses the original MM equation but it takes longer to run due to an additional iterative process that has to be made. NLU is also more susceptible to stabilization problems in the results. The linear model is a simplified version of the MM equation in which the solute uptake rate for the situation $C < C_{lim}$ is smaller when compared to the original nonlinear equation, it has no stabilization problems and runs faster. Therefore, the objective of this section is to analyze the differences between the results of the two models and check if those differences are significant. For that, four different general scenarios were chosen (using the parameters listed in Table 2, with loam soil) as listed below:

- Scenario 1: Medium root length density, High concentration and High potential transpiration (MrHcHt)
- Scenario 2: Medium root length density, High concentration and Low potential transpiration (MrHcLt)
- Scenario 3: Low root length density, High concentration and High potential transpiration (LrHcHt)
- Scenario 4: Medium root length density, Low concentration and High potential transpiration (MrLcHt)

In all simulated scenarios, the difference between LU and NLU models occurs only at values of solute concentration in soil water (C) below the threshold value C_{lim}. This is expected because of the nature of the piecewise MM equation used in the model. For both models, when solute concentration values are higher than C_2, all solute transport from soil to root is mostly driven by convection, therefore the uptake is passive only and active uptake is zero. With values of C between the two threshold values (C_2 and C_{lim}), the solute flux density is constant and NLU and LU are different only for C values lower than C_{lim} .

The difference between C outputs of LU and NLU was calculated as

$$diff = CLU - CNLU \tag{39}$$

where *CLU* and *CNLU* are the concentrations for LU and for NLU, respectively. When comparing differences in concentration between the two models, one has to be aware that $CNLU < CLU$ means that the uptake for NLU is greater than LU uptake since with a higher uptake, a higher amount of solute goes out from soil solution to inside the plant. Therefore, according to Equation (39), if $diff < 0$ then $CNLU > CLU$ and LU uptake is greater; if $diff > 0$ then $CNLU < CLU$ and NLU uptake is greater. Said that, we can see in Figure 2 that the uptake for NLU is greater then LU uptake at times when $C < C_{lim}$. This reflects a change also in the concentration profile for the latter times. Figure 3 shows the concentration profile at day 5 and the difference between CLU and CNLU through the profile. The higher NLU uptake increases the concentration gradient causing a higher solute flux (most diffusive since water flux is very small) from soil towards the root, resulting in a slightly higher concentration for NLU close to root surface ($diff. < 0$).

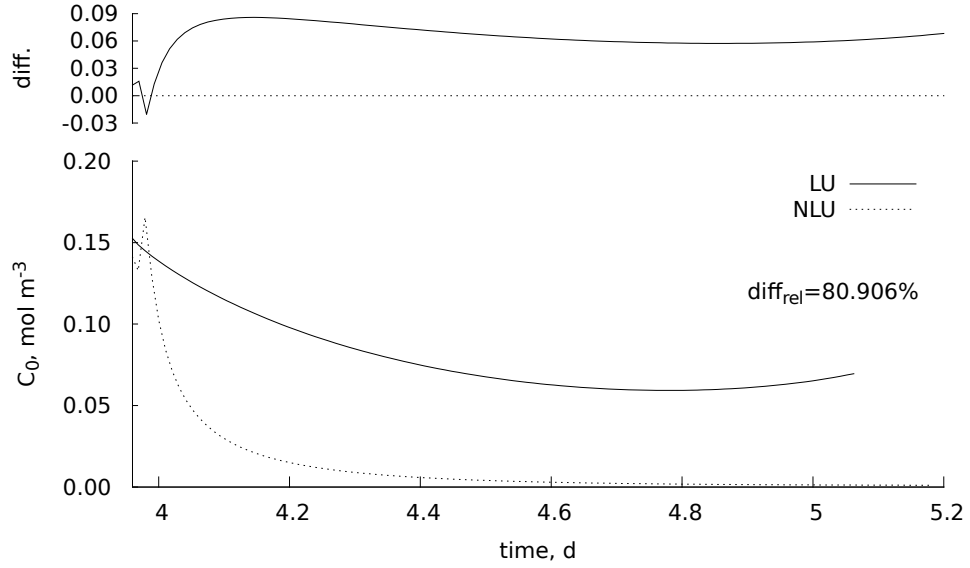

Figure 2 - Difference between the solute concentration in soil water at root surface (C_0) output for LU and NLU and C_0 as a function of time; and the relative difference – Scenario 1

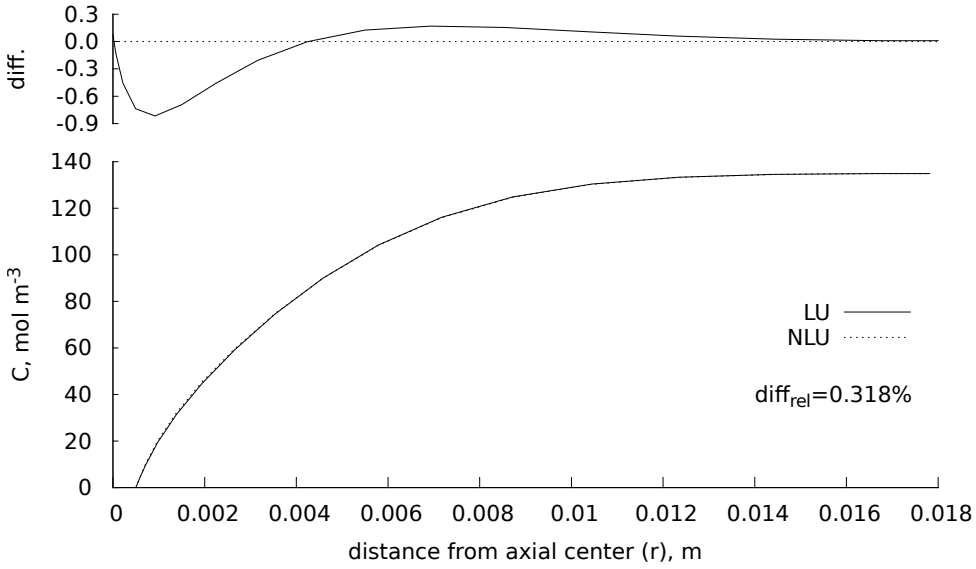

Figure 3 - Difference between the solute concentration in soil water (C) output for LU and NLU and C as a function of distance from axial center; and the relative difference – Scenario 1

Nevertheless, the difference between LU and NLU is negligible. A difference of 80.9% of concentration over time (Figure 2) corresponds to only 0.318% in the final concentration profile (Figure 3) because the uptake at times where $C < C_{lim}$ is really low. It can be seen at the cumulative uptake plot (Figure 4) the insignificant effect of this difference (for both models, the cumulative solute uptake is nearly the same).

Similar to Figures 2 and 3, the results of the relative accumulated error, according to Equation (38), were of 64.975% and 0.739%; 121.3% and 0.941%; 36.144% and 0.027% over time and distance for scenarios 2, 3 and 4, respectively.

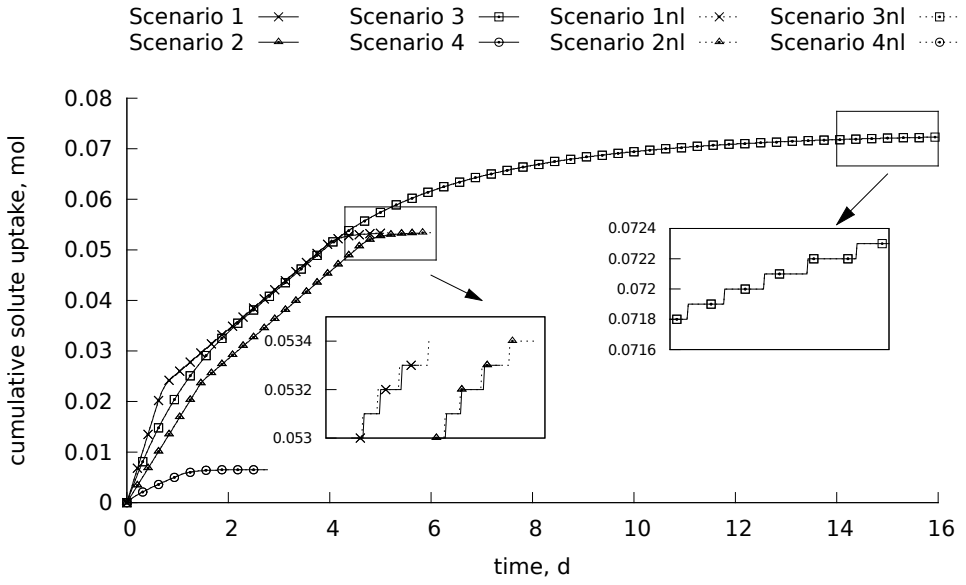

Figure 4 - Cumulative solute uptake as a function of time for all scenarios. Dashed lines represents the nonlinear model

The Mann–Whitney U test results corroborates with the differences analysis. Assuming a confidence interval of 95%, p-values below 0.05 indicates that the two models are different (one has greater values than the other), i.e. the hypothesis H_0 is rejected. Table 4 shows that, for scenarios 2, 3 and 4, concentration C_0 is significantly different for LU and NLU, but when analysing the cumulative uptake (for the same period of time where $C < C_{lim}$) the difference is not significant.

Table 4 - Mann–Whitney U test p-values for all scenarios. Confidence interval of 95%

Scenarios	p-**value concentration**	p-**value cum. uptake**
1	$2.2\ 10^{-16*}$	0.85
2	$1.5\ 10^{-12*}$	0.95
3	0.24	0.99
4	$2.2\ 10^{-16*}$	1.00

In addition, some part of the differences was due to stability problems with the numerical solution for NLU. The changing from equation 21 to equation 25 (change of boundary condition, from constant to nonlinear uptake rate) makes the numerical solution take some time to stabilize at the initial times. Many time and space steps combinations were used as an attempt to minimize the problem. Choosing a finer space discretization seems to decrease the stabilization problem but makes the simulation lasts longer. It needs to be found an optimal value for time and space step relation. Stabilization problems were not found in LU.

Since the differences between LU and NLU occurs for low concentration values and low solute flux, changes in relative transpiration are also negligible. The oscillation in the results due to the stabilization problem of the numerical solution is more likely to be noticed than the difference between the models. Figure 5 shows the relative transpiration as a function of time and details the part where the oscillation occurs for each scenario. The absolute and relative differences are all due to oscillation problem, since T_r turns out to be the same after complete convergence.

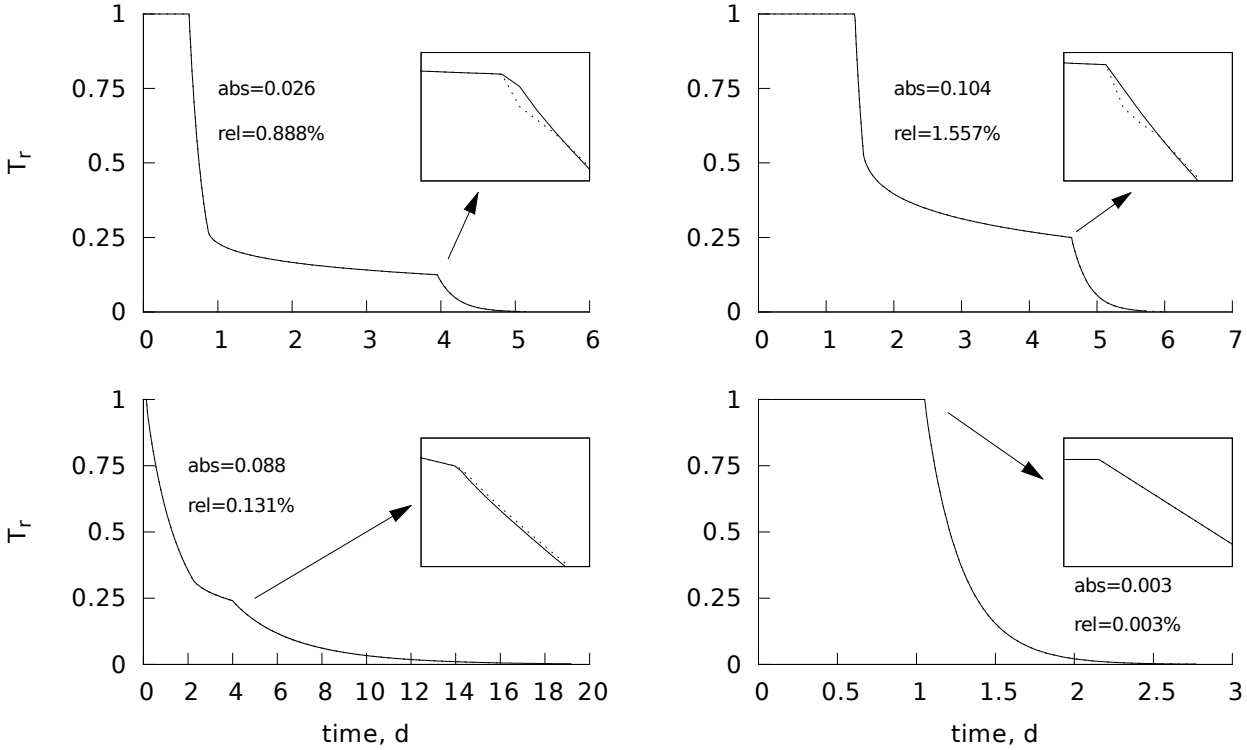

Figure 5 - Cumulative solute uptake as a function of time for all scenarios. Dashed lines represents the nonlinear model

Roose and Kirk (2009) stated that, for numerical solutions of convection-dispersion equation, the convective part might use an explicit scheme because convection, unlike diffusion, occurs only in one direction thus the solution at the following time step depends only on the values within the domain of influence of the previous time step. This set bounds on time and space steps, with a condition of stability given by $\frac{r_0 q_0 \Delta t}{D} < \Delta r$. As the proposed model uses a fully implicit scheme, that might be the cause of the stabilization problems.

The conclusion, since no significant difference between LU and NLU was found, can be either to choose LU as it takes less time to run and has no stabilization problems, or to choose NLU except for the cases in which the stability problem is significantly high. Note that this is the conclusion for those specific scenarios as the results can be significantly different for different soil and solute types.

4.2 Solute uptake models comparison

The scenario of this simulation is of loam soil, medium root length density, high potential transpiration and high initial concentration (Table 2). We compare all model types (no solute uptake – NU; constant – CU; linear – LU and nonlinear – NLU concentration dependent uptake rates). All simulations were made until the value of relative

transpiration was equal or less than 0.001. The time step is dynamical (depends on the number of iterations for water and solute equations) and was set to vary between 0.1 and 2 seconds. The simulation for NU ended within near 3 days; for CU, LU and NLU, about 5 days.

In NU, salt is transported to the roots by convection, causing an accumulation of solutes at root surface. As water flux towards the root starts to decrease, salt is transported slower and carried away from the roots by diffusion (Figure 6). Because of the accumulation of salt in the root surface, the total head becomes limiting very fast and the transpiration is reduced faster than the other models (Figure 9).

In CU, as the salt uptake rate is constant (Figure 8), the concentration at root surface will decrease only if the uptake rate is larger than convection to the root surface. In the simulation, it happens in about half of the first day (Figure 6). This is very dependent on the uptake rate and water flux since for different conditions, the outcome could be different. Once the concentration at root surface is zero, the root behaves as a zero-sink, taking up solute at the same rate as which it arrives at the root, keeping the concentration there zero.

In NLU, the concentration at root surface remains constant (Figure 6) until the convection to the root decreases as the water flux decreases (Figure 8). This behavior is really dependent of initial concentration and water flux values since, in this case, C_0 at the beginning of simulation is greater than C_2, thus the solute uptake equals the convection of solutes to the root. At around day 1, convection starts to decrease but the solute uptake is yet greater than the plant demand (I_m) due to convection. The solute uptake becomes constant (and equal to I_m) after concentration in root surface is less than C_2. This is clear in XXXFigure 3a, where osmotic head continues constant for a period of time after the beginning of the falling transpiration rate. At this point, active uptake starts since convection only is not capable to maintain solute uptake rate at I_m. The concentration keeps decreasing at this constant rate until its value is less than C_{lim}. It is assumed that, at this point, the uptake is not equal to the plant demand for solute (I_m) due to the concentration dependence of the MM equation (Figure 1). The water flux and the concentration are small as well as the active uptake, that can not maintain the uptake rate at I_m. Therefore, a second limiting condition occurs when $C < C_{lim}$ causing another fast decrease in transpiration (Figure 9). The calculated concentrations C_{lim} (Eq. (3)) and C_2 (Eq. (5)) depend on water flux and ion type (MM parameters I_m and K_m)

meaning that the results can be quite different for other ion types and different values of initial water content.

Figure 8 also shows the changes in solute flux at root surface for all models. At low concentrations (or at the second falling rate stage: $C < C_{lim}$), in NLU, the solute flux decreases gradually over time until the value of concentration is zero, where it will assume the zero-sink behavior.

The concentration profile through the distance from root axial center is shown in Figure 7. The different approaches (NU, CU and NLU) result in different final concentrations profiles. The concentration dependent model NLU takes up more solute from soil solution due to the higher uptake rate in the constant transpiration phase.

Figure 9 shows the relative transpiration as a function of time for the three model types. The proposed model is able to maintain the potential transpiration for a longer period of time due to the extraction by passive uptake only ($C > C_2$) that keeps the osmotic head constant, allowing pressure head to reach smaller values at the onset of the limiting hydraulic conditions, as can be seen in Figure 6.

Figure 9 shows that CU and NLU have a more negative pressure head value for the onset of limiting hydraulic condition when compared to NU due to solute uptake that causes a increase in osmotic head (becomes less negative) and, in turn, decreases pressure head. Thus, the first falling rate phase of relative transpiration extends in time. The solute uptake at the beginning of the simulation (for concentrations greater than C_2) caused a greater accumulation of solute in the plant and also influenced the final solute profile, in which LU and NLU have less solute left in the soil profile (Figure 13).

At the onset of the second falling rate phase ($C < C_{lim}$), water and solute fluxes decreases rapidly. In Figures XXX10 and 20 we can see that from day 4 to day 5, the fluxes are rapidly reduced, the water flux is near zero in the whole profile, meaning zero or really small convection. Thus, within this period, the transport of solute is made mainly by diffusion and the results of this diffusive transport can be visualized in Figures XXX17 and 18.

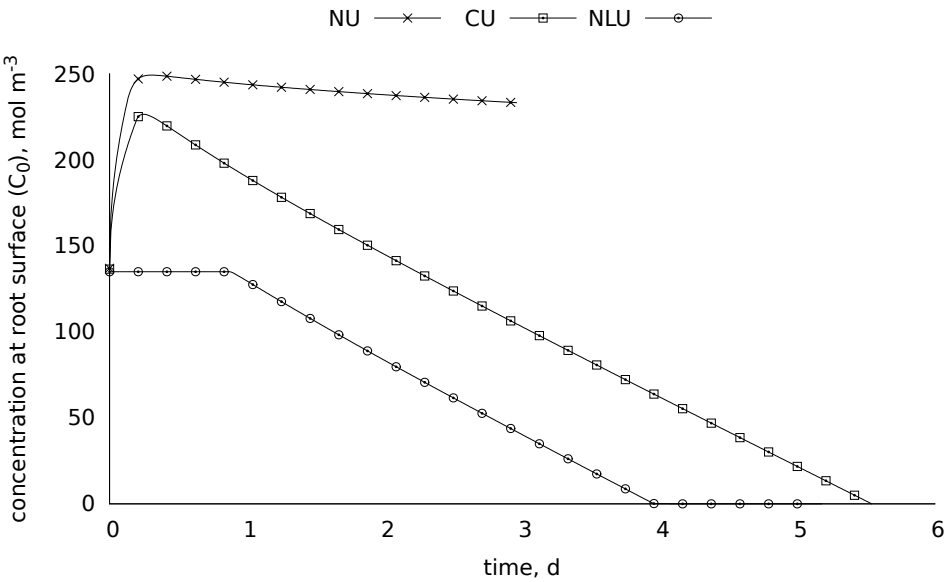

Figure 6 - Solute concentration in soil water at root surface as a function of time for no uptake (NU), constant (CU) and nonlinear (NLU) uptake models

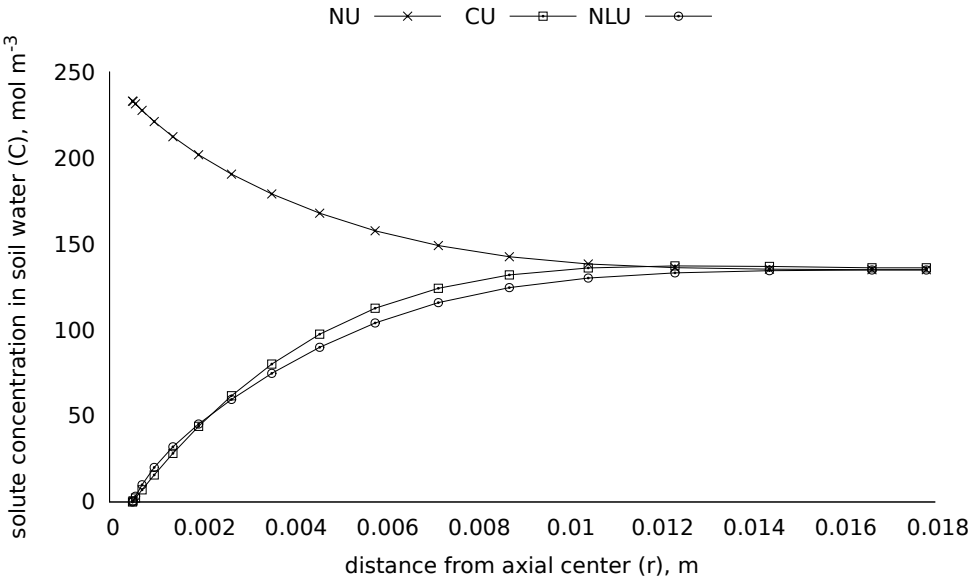

Figure 7 - Solute concentration in soil water as a function of distance from axial center for no uptake (NU), constant (CU) and nonlinear (NLU) uptake models

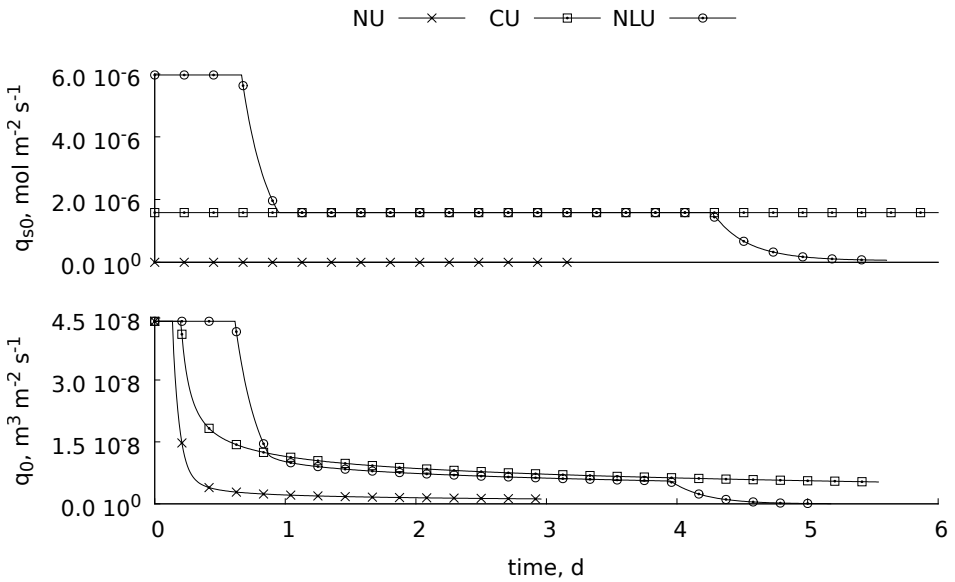

Figure 8 - Solute and water fluxes at root surface as a function of time for no uptake (NU), constant (CU) and nonlinear (NLU) uptake models

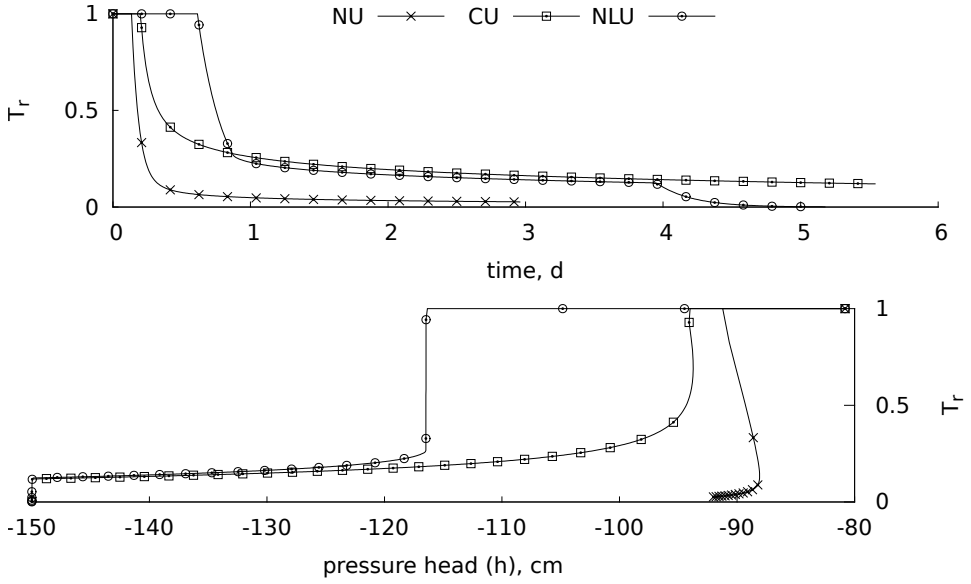

Figure 9 - Relative transpiration as a function of time and pressure head for no uptake (NU), constant (CU) and nonlinear (NLU) uptake models

5 CONCLUSION

The proposed model simulates the solute flux and root uptake considering a soil concentration dependent uptake. There was no significant difference between linear and nonlinear solutions for the simulated scenarios. The results of uptake for the proposed model showed that the limiting potential is reached at a higher pressure head, increasing the period of potential transpiration. It also showed a second limiting condition that happens at the time when $C < C_{lim}$ caused by a not sufficient supply of solute at the same rate of plant demand. The proposed model is also able to do a partition between active and passive uptake which will be important to simulate the plant stress due to ionic or osmotic components, according to the solute concentration inside the plant. Comparison between the numerical and the analytical solution proposed by Cushman is in process.

REFERENCES

DE JONG VAN LIER, Q.; METSELAAR, K.; VAN DAM, J.C. Root water extraction and limiting soil hydraulic conditions estimated by numerical simulation. **Vadose Zone Journal**, Soil Science Society, v. 5, n. 4, p. 1264–1277, 2006.

DE JONG VAN LIER, Q.; VAN DAM, J.C.; METSELAAR, K. Root water extraction under combined water and osmotic stress. **Soil Science Society of America Journal**, Soil Science Society, v. 73, n. 3, p. 862–875, 2009.

ROOSE, T.; KIRK, G. The solution of convection–diffusion equations for solute transport to plant roots. **Plant and soil**, Springer, v. 316, n. 1-2, p. 257–264, 2009.

WÖSTEN, J.; VEERMAN, G.; GROOT, W. D.; STOLTE, J. Waterretentie-en doorlatendheidskarakteristieken van boven-en ondergronden in nederland: de staringsreeks. Alterra, Research Instituut voor de Groene Ruimte, 2001.